Sensitivity of biological parameters on the operating diagrams for three-tiered model

Sarra Nouaoura, Radhouane Fekih-Salem, Tewfik Sari

Sensitivity of biological parameters on the operating diagrams for three-tiered model

Sarra Nouaoura * **Radhouane Fekih-Salem** **,**** **Tewfik Sari** ***

* *20 August 1955 University of Skikda, Mathematics Department, 21000, Skikda, Algeria. (e-mail: s.nouaoura@univ-skikda.dz).*
** *University of Tunis El Manar, National Engineering School of Tunis, LAMSIN, 1002, Tunis, Tunisia (e-mail: radhouane.fekih-salem@enit.utm.tn)*
*** *ITAP, Univ Montpellier, INRAE, Institut Agro, Montpellier, France. (e-mail: tewfik.sari@inrae.fr)*
**** *University of Monastir, Higher Institute of Computer Science of Mahdia, 5111, Mahdia, Tunisia*

Abstract: In this work, we considered the mechanistic model describing the anaerobic mineralization of chlorophenol in a three-tiered food-web, which is a six-dimensional system of ordinary differential equations. The aim of this work is to study the sensitivity of the process according to the biological parameters. To this end, we performed analytically the operating diagrams, using the mathematical analysis of this model obtained in our previous studies. These operating diagrams give the asymptotic behavior of the model with respect to the operating parameters and show the drastic change of the asymptotic behavior of the system on the biological parameters.

Keywords: Anaerobic mineralization, Bioenergy productions, Biological parameter, Operating diagram, Three-tiered food web, Wastewater treatment processes.

1. INTRODUCTION

Anaerobic digestion (AD) is an important process used for treating wastewater, municipal, industrial and agricultural wastes. It has the advantage of producing methane and hydrogen under appropriate conditions as a renewable energy source. The generic AD model No.1 (ADM1) developed in Batstone et al. (2002) is very complex because it is characterized by its extreme complexity with 32 state variables and a large number of parameters.

A simple two-step AD model (called AM2) developed in Bernard et al. (2001) provides satisfactory prediction of the AD process and demonstrates the ability to reproduce the experimental data and the dynamical behavior. Many papers in the literature have studied the AM2 model (see Bayen and Gajardo (2019); Fekih-Salem et al. (SIADS2021); Sari et al. (2012); Xu et al. (2011) and the reference therein).

A mathematical model of three-tiered microbial food-web has been proposed by Wade et al. (2016), by introducing an additional microorganism and substrate into a two-tiered feeding chain model considered by Xu et al. (2011). Several authors studied the three-tiered model, see El-Hajji et al. (2017); Nouaoura et al. (DcDsB2020,S); Sari and Wade (2017); Sobieszek et al. (2020); Wade et al. (2016).

Using specific growth rates, Wade et al. (2016) have proven that the model can have up to eight steady states. Several operating diagrams, which shows the dynamic behavior of the system with respect to the four operating parameters (the dilution rate and the three input concentrations of the substrates) such that the values of the biological parameters are fixed have been constructed numerically and they did not depict all the behavior of the model.

Sari and Wade (2017) have considered the case with only the chlorophenol inflowing concentration has been taken into account and general growth rates. The operating diagrams were obtained analytically in the case without maintenance and numerically in the case with maintenance. Adding the maintenance terms, they highlighted by a numerical stability analysis the presence of the region of instability of the positive steady state with the appearance of a stable limit cycle via a Hopf bifurcation. These phenomena were not depicted in Wade et al. (2016). Indeed, they were proved theoretically in Sobieszek et al. (2020) in the case neglecting maintenance.

In Nouaoura et al. (DcDsB2020), we have extended the results of Sari and Wade (2017) by considering the inflow of the three substrate concentrations. The necessary and sufficient existence conditions of the steady states are analytically performed in the case with maintenance. The necessary and sufficient local stability conditions are performed analytically when maintenance is excluded. Then, these results of local stability are extended in Nouaoura et al. (Siap2021) to the case where maintenance is included. The one parameter bifurcation diagrams of the three-tiered model presented in Nouaoura et al. (Siap2021,D) were analytically constructed in the cases with and without maintenance. They show that the model has in both cases rich dynamics including bistability, coexistence and occurrence of the limit cycle due to supercritical Hopf bifurcation.

Recently, in Nouaoura et al. (Preprint2021), we have performed theoretically the operating diagrams by using the analytical results of the existence and stability conditions in Nouaoura et al. (Siap2021,D). We highlighted the impact of the maintenance terms and the importance of the operating parameters on the asymptotic behavior of the model. We have compared our results with the findings of previous numerical study in Wade et al. (2016) where several regions have been omitted.

In this work, we reconsider the three-tiered model proposed in Wade et al. (2016). The first contribution is the determination of the operating diagrams analytically when only the chlorophenol is in the input of the bioreactor and in both cases with and without decay terms, to compare with the numerically operating diagrams obtained in Sari and Wade (2017). The second contribution is to highlight the sensitivity of the biological parameter on the qualitative behavior of the system confirming the findings of previous numerical analysis in Sari and Wade (2017).

The paper is organized as follows. In section 2, we present the mathematical model of three-tiered microbial species of Wade et al. (2016). Next, in section 3, we describe analytically the operating diagrams in both cases with and without maintenance terms. Finally, we discuss our results and we give some conclusions in section 4. In Appendix A, we present the change of variables that are used to simplify the analysis of the general model and we describe the results of Nouaoura et al. (Siap2021,D) on the existence and local stability of the steady states. The equations of the curves that delimit the regions of the operating diagrams are provided in Appendix B.

2. MATHEMATICAL MODEL

The three-tiered model, considered in Wade et al. (2016), can be written as follows:

$$\begin{cases} \dot{X}_{\mathrm{ch}} &= (Y_{\mathrm{ch}} f_0\left(S_{\mathrm{ch}}, S_{\mathrm{H}_2}\right) - D - k_{\mathrm{dec,ch}}) X_{\mathrm{ch}} \\ \dot{X}_{\mathrm{ph}} &= (Y_{\mathrm{ph}} f_1\left(S_{\mathrm{ph}}, S_{\mathrm{H}_2}\right) - D - k_{\mathrm{dec,ph}}) X_{\mathrm{ph}} \\ \dot{X}_{\mathrm{H}_2} &= (Y_{\mathrm{H}_2} f_2\left(S_{\mathrm{H}_2}\right) - D - k_{\mathrm{dec,H}_2}) X_{\mathrm{H}_2} \\ \dot{S}_{\mathrm{ch}} &= D\left(S_{\mathrm{ch}}^{\mathrm{in}} - S_{\mathrm{ch}}\right) - f_0\left(S_{\mathrm{ch}}, S_{\mathrm{H}_2}\right) X_{\mathrm{ch}} \\ \dot{S}_{\mathrm{ph}} &= D\left(S_{\mathrm{ph}}^{\mathrm{in}} - S_{\mathrm{ph}}\right) + \frac{224}{208}\left(1 - Y_{\mathrm{ch}}\right) f_0\left(S_{\mathrm{ch}}, S_{\mathrm{H}_2}\right) X_{\mathrm{ch}} \\ & \quad - f_1\left(S_{\mathrm{ph}}, S_{\mathrm{H}_2}\right) X_{\mathrm{ph}} \\ \dot{S}_{\mathrm{H}_2} &= D\left(S_{\mathrm{H}_2}^{\mathrm{in}} - S_{\mathrm{H}_2}\right) - \frac{16}{208} f_0\left(S_{\mathrm{ch}}, S_{\mathrm{H}_2}\right) X_{\mathrm{ch}} \\ & \quad + \frac{32}{224}(1 - Y_{\mathrm{ph}}) f_1\left(S_{\mathrm{ph}}, S_{\mathrm{H}_2}\right) X_{\mathrm{ph}} - f_2(S_{\mathrm{H}_2}) X_{\mathrm{H}_2}, \end{cases} \tag{1}$$

where S_{ch}, S_{ph} and S_{H_2} are the chlorophenol, phenol and hydrogen substrate concentrations, respectively; X_{ch}, X_{ph} and X_{H_2} are the chlorophenol, phenol and hydrogen degrader concentrations; D is the dilution rate; f_i, $i = 0, 1, 2$ are the specific growth rates; $S_{\mathrm{ch}}^{\mathrm{in}}, S_{\mathrm{ph}}^{\mathrm{in}}$ and $S_{\mathrm{H}_2}^{\mathrm{in}}$ are the inflowing concentrations in the chemostat; $k_{\mathrm{dec,ch}}, k_{\mathrm{dec,ph}}$ and $k_{\mathrm{dec,H}_2}$ are the maintenance (or decay) rates; Y_{ch}, Y_{ph} and Y_{H_2} are the yield coefficients. The value $224/208\left(1 - Y_{\mathrm{ch}}\right)$ is the fraction of chlorophenol converted to phenol, $32/224\left(1 - Y_{\mathrm{ph}}\right)$ is the fraction of phenol that is transformed to hydrogen and $16/208$ is the fraction of hydrogen consumed by the chlorophenol degrader X_{ch}.

The growth functions take the following form:

$$\begin{aligned} f_0\left(S_{\mathrm{ch}}, S_{\mathrm{H}_2}\right) &= \frac{k_{m,\mathrm{ch}} S_{\mathrm{ch}}}{K_{S,ch} + S_{\mathrm{ch}}} \frac{S_{H_2}}{K_{S,\mathrm{H}_2,\mathrm{c}} + S_{\mathrm{H}_2}}, \\ f_1\left(S_{\mathrm{ph}}, S_{\mathrm{H}_2}\right) &= \frac{k_{m,\mathrm{ph}} S_{\mathrm{ph}}}{K_{S,\mathrm{ph}} + S_{\mathrm{ph}}} \frac{1}{1 + S_{\mathrm{H}_2}/K_{I,\mathrm{H}_2}}, \\ f_2\left(S_{\mathrm{H}_2}\right) &= \frac{k_{m,\mathrm{H}_2} S_{\mathrm{H}_2}}{K_{S,\mathrm{H}_2} + S_{\mathrm{H}_2}}. \end{aligned} \tag{2}$$

The case with $S_{\mathrm{ph}}^{\mathrm{in}} > 0$ and $S_{\mathrm{H}_2}^{\mathrm{in}} > 0$ was analyzed in Nouaoura et al. (Siap2021,D) using a general class of growth functions. Following Sari and Wade (2017), we restrict our analysis to the case where we only the chlorophenol input substrate is added to the system, that is, $S_{\mathrm{ch}}^{\mathrm{in}} > 0$, $S_{\mathrm{ph}}^{\mathrm{in}} = S_{\mathrm{H}_2}^{\mathrm{in}} = 0$. In this case, system (1) can have up to three steady states labeled E_1, E_2 and E_3 and defined as follows:

- E_0: the washout steady state where all populations are extinct.
- E_1: $X_{\mathrm{ch}} > 0$, $X_{\mathrm{ph}} > 0$ and $X_{\mathrm{H}_2} = 0$, where only the hydrogenotrophic methanogens are washed out.
- E_2: $X_{\mathrm{ch}} > 0$, $X_{\mathrm{ph}} > 0$ and $X_{\mathrm{H}_2} > 0$, where all three populations are maintained.

These steady states are denoted by SS1, SS2 and SS3 in Sari and Wade (2017), and by SS1, SS4 and SS6 in Wade et al. (2016), respectively. From Nouaoura et al. (DcDsB2020), the components of these steady states are given in Table A.1. The conditions of their existence and stability are provided in Table A.2.

Remark 1. The steady state E_0 always exists. There exist at most two steady states of the form E_1, that we denote by E_1^1 and E_1^2. The steady state E_2 is unique if it exists (see Sari and Wade (2017) or Nouaoura et al. (DcDsB2020)).

3. OPERATING DIAGRAMS

The operating diagrams show how behaves the system when the operating parameters D and $S_{\mathrm{ch}}^{\mathrm{in}}$ are varying in (1). To plot the operating diagrams, we must fix the values of the biological parameters which are provided in Table 1 of Wade et al. (2016). From Table A.2, we define in Table B.1 the curves Γ_i, $i = 1, \ldots, 5$ which delimite the different regions of the $\left(S_{\mathrm{ch}}^{\mathrm{in}}, D\right)$-plane. These curves separate the operating space $\left(S_{\mathrm{ch}}^{\mathrm{in}}, D\right)$ into five regions, denoted $\mathcal{J}_j$, $j = 1, \ldots, 5$.

Using our result in Nouaoura et al. (Preprint2021), we recall the existence and the stability of the steady states of (1) according to the five regions $\mathcal{J}_i$, $i = 1, \ldots, 5$, of the operating diagrams determined in Table 1.

In our previous study, Nouaoura et al. (Preprint2021), we have extended in case where $S_{\mathrm{ph}}^{\mathrm{in}} > 0$ and/or $S_{\mathrm{H}_2}^{\mathrm{in}} > 0$. Following Sari and Wade (2017), we plot in the following the operating diagrams corresponding to three cases which obtained with the numerical parameter values of $K_{\mathrm{S,H_2,c}}$ given in Table B.2, in the cases with and without maintenance.

Table 1. Existence and stability of steady states in the regions of the operating diagrams. The letter S (resp. U) means that the corresponding steady state is LES (resp. unstable). No letter means that the steady state does not exist.

Region	E_0	E_1^1	E_1^2	E_2	Color
$\mathcal{J}_1$	S				Red
$\mathcal{J}_2$	S	U	S		Green
$\mathcal{J}_3$	S	U	U	S	Yellow
$\mathcal{J}_4$	S	U	U		Blue
$\mathcal{J}_5$	S	U	U	U	Blueviolet

3.1 Operating diagrams: case (a)

First, we consider the case of Fig. 4 in Sari and Wade (2017) where $K_{\mathrm{S,H_2,c}} = 10^{-6}$. The operating diagram in the plane $\left(S_{\mathrm{ch}}^{\mathrm{in}}, D\right)$ is shown in Fig. 1. Fig. 1(i) looks very similar to Fig. 1(ii) except near of the origin. However, there are no new regions that appear under the influence of the maintenance terms. Fig. 1(ii) highlights the existence of the region $\mathcal{J}_5$ of instability of E_2 which was already detected in Sari and Wade (2017), a fact that was not reported in Wade et al. (2016). Note that, each region that has a different asymptotic behavior is colored by a distinct color as in Sari and Wade (2017).

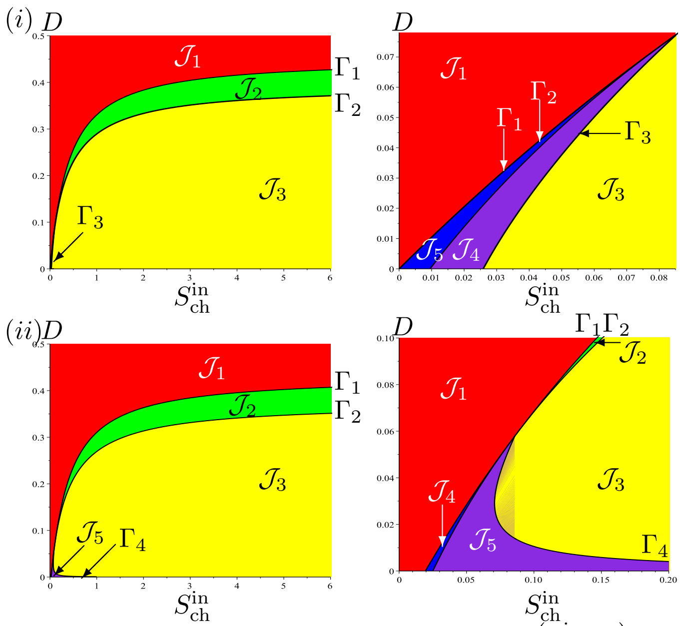

Fig. 1. Operating diagrams in the plane $\left(S_{\mathrm{ch}}^{\mathrm{in}}, D\right)$, for case (a): (i) case without maintenance, on the right its magnification for $D \in [0, 0.078]$, (ii) case with maintenance, on the right its magnification for $D \in [0, 0.1]$.

Therefore, our theoretical study shows the same behavior as Figs. 8 and 9 in Sari and Wade (2017) and confirms the numerical findings presented in Sari and Wade (2017), in the both cases with and without maintenance.

3.2 Operating diagrams: case (b)

In the following, we study the operating diagrams of system (1) in the $\left(S_{\mathrm{ch}}^{\mathrm{in}}, D\right)$-plane by assuming a small increase to the biological parameter $K_{\mathrm{S,H_2,c}} = 4 \times 10^{-6}$ as in Fig. 5 of Sari and Wade (2017). In the case with maintenance, the value of $S_{\mathrm{ch}}^{\mathrm{in}}$, in which the positive steady state E_2 is destabilized is greater than in the case without maintenance, as shown in the operating diagram presented in Fig. 2.

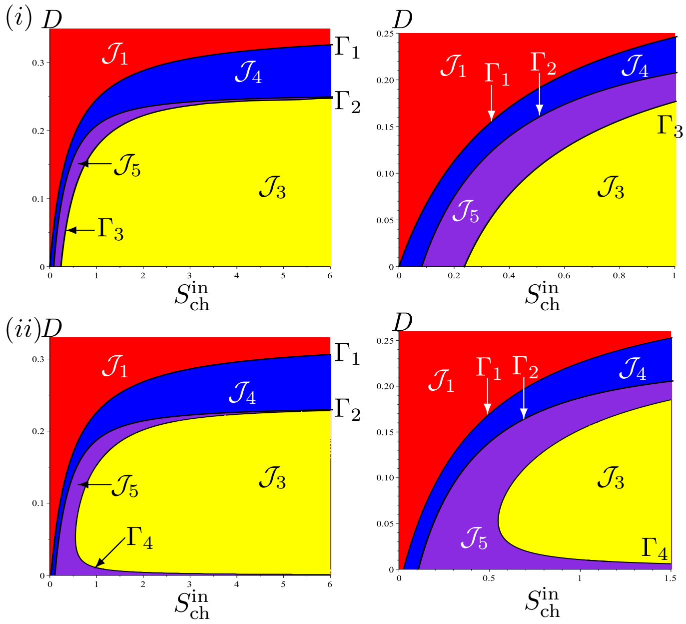

Fig. 2. Operating diagrams in the plane $\left(S_{\mathrm{ch}}^{\mathrm{in}}, D\right)$, for case (b): (i) case without maintenance and on the right its magnification for $D \in [0, 0.25]$, (ii) case with maintenance and on the right its magnification for $D \in [0, 0.26]$.

Increasing $K_{\mathrm{S,H_2,c}}$ leads to the disappearance of the bistability region $\mathcal{J}_2$ of the steady states E_0 and E_1 and to changes in the size of the existence and stability regions of the other steady states. Actually, the behavior of the system when $K_{\mathrm{S,H_2,c}} = 4 \times 10^{-6}$ was already clarified in Sari and Wade (2017), where the instability of E_2 has been studied numerically in both cases with and without maintenance. In fact, Fig. 2 is the same as Fig. 11 in Sari and Wade (2017), which is obtained analytically. However, although Fig. 2 shows the same behavior as Fig. 11 in Sari and Wade (2017) achieved only numerically. Thus, our theoretical study confirms the numerical findings presented in Sari and Wade (2017), in the both cases that the maintenance is excluded and included in the system.

3.3 Operating diagrams: case (c)

In the following, we analyze the effect of the biological parameter $K_{\mathrm{S,H_2,c}}$ on the behavior of the process in both case with and without maintenance. By comparing with the results obtained in the previous subsection, we increase the half-saturation constant $K_{\mathrm{S,H_2,c}}$ of the chlorophenol degrader on the hydrogen from 4×10^{-6} to 6×10^{-6}. The operating diagrams shown in Fig. 3 produce similar results as shown in the comparison of Fig. 2 in both cases, with variations only in their shape and extent. However, Fig. 3 shows the effect of the parameter $K_{\mathrm{S,H_2,c}}$ on the size of the regions, where the regions $\mathcal{J}_3$ and $\mathcal{J}_5$ diminish in the cases with and without decay terms.

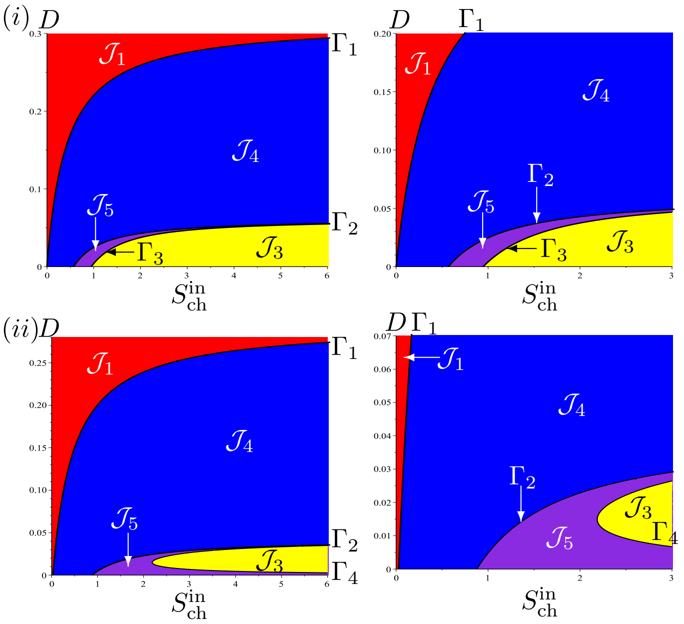

Fig. 3. Operating diagrams in the plane $\left(S_{\rm ch}^{\rm in}, D\right)$, for case (b): (i) case without maintenance and on the right its magnification for $D \in [0, 0.2]$, (ii) case with maintenance and on the right its magnification for $D \in [0, 0.07]$.

3.4 Operating diagrams: case (d)

Increasing once again the biological parameter $K_{\rm S,H_2,c}$, when we consider $K_{\rm S,H_2,c} = 7 \times 10^{-6}$ corresponding to case (c) in Sari and Wade (2017). The operating diagram in the plane $\left(S_{\rm ch}^{\rm in}, D\right)$ is shown in Fig. 4. We have seen in the operating diagram presented in Fig. 4 that the steady states E_1 never stable and E_2 never exist, since I_2 is empty in both cases with and without maintenance.

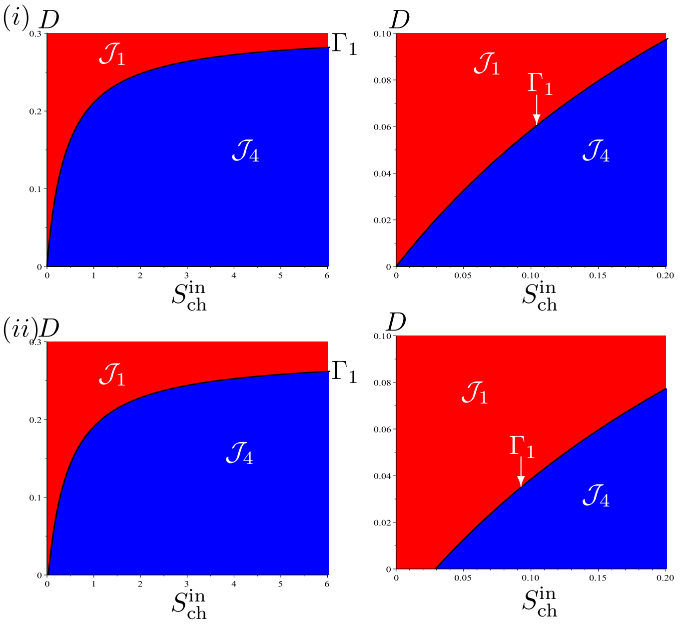

Fig. 4. Operating diagrams in the plane $\left(S_{\rm ch}^{\rm in}, D\right)$, for case (d): (i) case without maintenance and on the right its magnification for $D \in [0, 0.1]$, (ii) case with maintenance and on the right its magnification for $D \in [0, 0.1]$.

Fig. 4 is the same as Fig. 12 in Sari and Wade (2017), which is obtained analytically. Thus, our theoretical study confirms the numerical results given in Sari and Wade (2017), in the both cases with and without maintenance, such as Fig. 4 shows the same behavior as Fig. 12 in Sari and Wade (2017) achieved only numerically.

4. CONCLUSION

In this work, we gave an analytical study of the operating diagrams of the three-tiered microbial model (1) developed in Wade et al. (2016). Considering only the chlorophenol input substrate concentration, we compare our results with those obtained numerically in Sari and Wade (2017). Our main aim was to present the mathematical analysis of the operating diagrams and to illustrate its dependence on the biological parameters of the process.

Our theoretical study of the operating diagrams in the $\left(S_{\rm ch}^{\rm in}, D\right)$-plane of Figs. 1 to 4 show the same number of regions in both cases with and without maintenance, with variations only in their shape and extension. Moreover, it confirmes the numerical results of Sari and Wade (2017). In fact, our analytical operating diagrams in the case with only chlorophenol addition in the input show that all asymptotic behaviors were reported in Sari and Wade (2017). Thus, the mathematical analysis of the operating diagram remains the only way to ensure the accuracy of the results. Our study show the sensibility of the asymptotic behavior of the process on the biological parameters.

Appendix A. MATHEMATICAL ANALYSIS OF THE MODEL

In this section, we recall from Nouaoura et al. (Siap2021,D) the main results of existence and stability of all steady states of system (1). Following Sari and Wade (2017), we can rescale model (1) to reduce the number of yield parameters and ease the mathematical analysis. We use the following change of variables:

$$\begin{aligned} x_0 &= \frac{Y}{Y_0} X_{\rm ch}, \quad x_1 = \frac{Y_4}{Y_1} X_{\rm ph}, \quad x_2 = \frac{1}{Y_2} X_{\rm H_2}, \\ s_0 &= Y S_{\rm ch}, \quad s_1 = Y_4 S_{\rm ph}, \quad s_2 = S_{\rm H_2}, \end{aligned} \tag{A.1}$$

where the yield coefficients are

$$Y_0 = Y_{\rm ch}, \ Y_1 = Y_{\rm ph}, \ Y_2 = Y_{\rm H_2},$$
$$Y_3 = \frac{224}{208}(1 - Y_0), \ Y_4 = \frac{32}{224}(1 - Y_1),$$

with $Y = Y_3 Y_4$ and $\omega = \frac{16}{208Y}$. The inflowing concentrations are:

$$s_0^{\rm in} = Y S_{\rm ch}^{\rm in}, \quad s_1^{\rm in} = Y_4 S_{\rm ph}^{\rm in}, \quad s_2^{\rm in} = S_{\rm H_2}^{\rm in}, \tag{A.2}$$

the death rates are $a_0 = k_{\rm dec,ch}$, $a_1 = k_{\rm dec,ph}$ and $a_2 = k_{\rm dec,H_2}$. Under the scaling (A.1), the growth functions become:

$$\begin{aligned} \mu_0(s_0, s_2) &= \frac{m_0 s_0}{K_0 + s_0} \frac{s_2}{L_0 + s_2}, \\ \mu_1(s_1, s_2) &= \frac{m_1 s_1}{K_1 + s_1} \frac{1}{1 + s_2/K_I}, \mu_2(s_2) = \frac{m_2 s_2}{K_2 + s_2}, \end{aligned} \tag{A.3}$$

where

$m_0 = Y_0 k_{m,\mathrm{ch}}, K_0 = Y K_{S,\mathrm{ch}}, L_0 = K_{S,\mathrm{H}_2,\mathrm{c}}, m_1 = Y_1 k_{m,\mathrm{ph}},$
$K_1 = Y_4 K_{S,\mathrm{ph}}, K_I = K_{I,\mathrm{H}_2}, m_2 = Y_2 k_{m,\mathrm{H}_2}, K_2 = K_{S,\mathrm{H}_2}.$

Using the change of variables (A.1) and (A.2), and Table 2 in Nouaoura et al. (DcDsB2020), we can recall now the steady states of system (1) in Table A.1. From Table 3 in Nouaoura et al. (Siap2021) and the change of variables (A.2), all necessary and sufficient existence and stability conditions of the steady states of (1) in the case with maintenance are stated in Table A.2.

Table A.1. The steady states of (1). The function μ_i are given by (A.3). The function M_i, ψ_i and Ψ are given in Table 11 of Nouaoura et al. (DcDsB2020). For the general case, the functions are given in Table 1 of Nouaoura et al. (DcDsB2020).

	s_0, s_1, s_2	x_0, x_1, x_2
E_0	$s_0 = YS_{\mathrm{ch}}^{\mathrm{in}}$, $s_1 = Y_4 S_{\mathrm{ph}}^{\mathrm{in}}$, $s_2 = S_{\mathrm{H}_2}^{\mathrm{in}}$	$x_0 = 0$, $x_1 = 0$, $x_2 = 0$
E_1	$s_2 = s_2\left(D, S_{\mathrm{ch}}^{\mathrm{in}}, S_{\mathrm{ph}}^{\mathrm{in}}, S_{\mathrm{H}_2}^{\mathrm{in}}\right)$ is a solution of $\Psi(s_2, D) = (1-\omega)YS_{\mathrm{ch}}^{\mathrm{in}} + Y_4 S_{\mathrm{ph}}^{\mathrm{in}} + S_{\mathrm{H}_2}^{\mathrm{in}}$ $s_0 = M_0(D + a_0, s_2)$, $s_1 = M_1(D + a_1, s_2)$	$x_0 = \frac{D}{D+a_0}\left(YS_{\mathrm{ch}}^{\mathrm{in}} - s_0\right)$, $x_1 = \frac{D}{D+a_1}(YS_{\mathrm{ch}}^{\mathrm{in}} + Y_4 S_{\mathrm{ph}}^{\mathrm{in}} - s_0 - s_1)$, $x_2 = 0$
E_2	$s_0 = M_0(D + a_0, M_2(D + a_2))$, $s_1 = M_1(D + a_1, M_2(D + a_2))$, $s_2 = M_2(D + a_2)$	$x_0 = \frac{D}{D+a_0}\left(YS_{\mathrm{ch}}^{\mathrm{in}} - s_0\right)$, $x_1 = \frac{D}{D+a_1}(YS_{\mathrm{ch}}^{\mathrm{in}} + Y_4 S_{\mathrm{ph}}^{\mathrm{in}} - s_0 - s_1)$ $x_2 = \frac{D}{D+a_2}((1-\omega)(YS_{\mathrm{ch}}^{\mathrm{in}} - s_0) + Y_4 S_{\mathrm{ph}}^{\mathrm{in}} + S_{\mathrm{H}_2}^{\mathrm{in}} - s_1 - s_2)$,

Table A.2. Case of maintenance: necessary and sufficient existence and local stability conditions of steady states of (1). The functions c_3, c_5, r_3 and r_5 are given in Table 2 in Nouaoura et al. (Siap2021). All other functions are given in Table 8 of Nouaoura et al. (Siap2021).

	Existence conditions	Stability conditions
E_0	always exists	$\mu_0\left(S_{\mathrm{ch}}^{\mathrm{in}} Y, S_{\mathrm{H}_2}^{\mathrm{in}}\right) < D + a_0$, $\mu_1\left(S_{\mathrm{ph}}^{\mathrm{in}} Y_4, S_{\mathrm{H}_2}^{\mathrm{in}}\right) < D + a_1$, $\mu_2\left(S_{\mathrm{H}_2}^{\mathrm{in}}\right) < D + a_2$
E_1	$\phi_1(D) \leq (1-\omega)YS_{\mathrm{ch}}^{\mathrm{in}} + Y_4 S_{\mathrm{ph}}^{\mathrm{in}} + S_{\mathrm{H}_2}^{\mathrm{in}}$, $S_{\mathrm{ch}}^{\mathrm{in}} Y > M_0(D + a_0, s_2)$, $S_{\mathrm{ch}}^{\mathrm{in}} Y + S_{\mathrm{ph}}^{\mathrm{in}} Y_4 > M_0(D + a_0, s_2) + M_1(D + a_1, s_2)$, with s_2 solution of equation $\Psi(s_2) = (1-\omega)S_{\mathrm{ch}}^{\mathrm{in}} Y + S_{\mathrm{ph}}^{\mathrm{in}} Y_4 + S_{\mathrm{H}_2}^{\mathrm{in}}$	$\phi_2(D) > (1-\omega)S_{\mathrm{ch}}^{\mathrm{in}} Y + S_{\mathrm{ph}}^{\mathrm{in}} Y_4 + S_{\mathrm{H}_2}^{\mathrm{in}}$, $\frac{\partial \Psi}{\partial s_2}(s_2, D) > 0$ and $\phi_3(D) > 0$
E_2	$\phi_2(D) < (1-\omega)S_{\mathrm{ch}}^{\mathrm{in}} Y + S_{\mathrm{ph}}^{\mathrm{in}} Y_4 + S_{\mathrm{H}_2}^{\mathrm{in}}$, $S_{\mathrm{ch}}^{\mathrm{in}} Y > \varphi_0(D)$, $S_{\mathrm{ch}}^{\mathrm{in}} Y + S_{\mathrm{ph}}^{\mathrm{in}} Y_4 > \varphi_0(D) + \varphi_1(D)$	$c_3 > 0$, $c_5 > 0$, $r_4 > 0$, $r_5 > 0$

Remark 2. In the case without maintenance, the necessary and sufficient conditions of existence and local stability can be deduced from Table A.2 by taking $a_i = 0$, except for the stability condition of SS6 which is given by

$$\phi_3(D) \geq 0 \text{ or } \phi_3(D) < 0, \phi_4(D, S_{\mathrm{ch}}^{\mathrm{in}}, S_{\mathrm{ph}}^{\mathrm{in}}, S_{\mathrm{H}_2}^{\mathrm{in}}) > 0, \quad \text{(A.4)}$$

where the function ϕ_3 is defined in Table 1 in Nouaoura et al. (DcDsB2020) and ϕ_4 is defined by:

$$\begin{aligned}\phi_4(D, S_{\mathrm{ch}}^{\mathrm{in}}, S_{\mathrm{ph}}^{\mathrm{in}}, S_{\mathrm{H}_2}^{\mathrm{in}}) = \; & (EIx_0x_2 + EG\phi_3(D)x_0x_1)(Ix_2 + \\ & (G+H)x_1 + (E+\omega F)x_0) + (Ix_2 \\ & +(G+H)x_1 + \omega F x_0)GIx_1x_2,\end{aligned} \quad \text{(A.5)}$$

with

$$E = \frac{\partial \mu_0}{\partial s_0}(s_0, s_2),\; F = \frac{\partial \mu_0}{\partial s_2}(s_0, s_2),\; G = \frac{\partial \mu_1}{\partial s_1}(s_1, s_2),$$
$$H = -\frac{\partial \mu_1}{\partial s_2}(s_1, s_2),\; I = \frac{d\mu_2}{ds_2}(s_2).$$

Appendix B. TABLES

Table B.1. Definitions of the surfaces Γ_i, $i = 1, \ldots, 5$.

$\Gamma_1 =$	$\left\{\left(S_{\mathrm{ch}}^{\mathrm{in}}, S_{\mathrm{ph}}^{\mathrm{in}}, S_{\mathrm{H}_2}^{\mathrm{in}}, D\right),\; S_{\mathrm{ch}}^{\mathrm{in}} Y(1-\omega) = \phi_1(D) - S_{\mathrm{ph}}^{\mathrm{in}} Y_4 - S_{\mathrm{H}_2}^{\mathrm{in}}\right\}$
$\Gamma_2 =$	$\left\{\left(S_{\mathrm{ch}}^{\mathrm{in}}, S_{\mathrm{ph}}^{\mathrm{in}}, S_{\mathrm{H}_2}^{\mathrm{in}}, D\right),\; S_{\mathrm{ch}}^{\mathrm{in}} Y(1-\omega) = \phi_2(D) - S_{\mathrm{ph}}^{\mathrm{in}} Y_4 - S_{\mathrm{H}_2}^{\mathrm{in}}\right\}$
$\Gamma_3 =$	$\left\{\left(S_{\mathrm{ch}}^{\mathrm{in}}, S_{\mathrm{ph}}^{\mathrm{in}}, S_{\mathrm{H}_2}^{\mathrm{in}}, D\right),\; \phi_4\left(D, S_{\mathrm{ch}}^{\mathrm{in}}, S_{\mathrm{ph}}^{\mathrm{in}}, S_{\mathrm{H}_2}^{\mathrm{in}}\right) = 0\right\}$
$\Gamma_4 =$	$\left\{\left(S_{\mathrm{ch}}^{\mathrm{in}}, S_{\mathrm{ph}}^{\mathrm{in}}, S_{\mathrm{H}_2}^{\mathrm{in}}, D\right),\; r_5\left(D, S_{\mathrm{ch}}^{\mathrm{in}}, S_{\mathrm{ph}}^{\mathrm{in}}, S_{\mathrm{H}_2}^{\mathrm{in}}\right) = 0\right\}$

Table B.2. Parameter values of the biological parameter $K_{S,H_2,c}$ for cases (a), (b), (c) and (d).

Cases	(a)	(b)	(c)	(d)
$K_{S,H_2,c}$	10^{-6}	4×10^{-6}	6×10^{-6}	7×10^{-6}

ACKNOWLEDGEMENTS

This work was supported by the Euro-Mediterranean research network TREASURE (https://www6.inrae.fr/treasure).

REFERENCES

D.J. Batstone, J. Keller, I. Angelidaki, S.V. Kalyhuzhnyi, S.G. Pavlosthathis, A. Rozzi, W.T.M Sanders, H. Siegrist and V.A. Vavilin, The IWA Anaerobic Digestion Model No 1 (ADM1), *Water Sci Technol*, 45, pages 66–73, 2002.

O. Bernard, Z. Hadj-Sadok, D. Dochain, A. Genovesi and J-P. Steyer, Dynamical model development and parameter identification for an anaerobic wastewater treatment process, *Biotechnol. Bioeng*, 75, pages 424–438, 2001.

T. Bayen and, P. Gajardo, On the steady state optimization of the biogas production in a two-stage anaerobic digestion model, *Math. Biol. J*, 78, pages 1067–1087, 2019.

M. El-Hajji, N. Chorfi and M. Jleli, Mathematical modelling and analysis for a three-tiered microbial food web in a chemostat, *Electron. J. Differential Equations*, 255, 2017.

R. Fekih-Salem, Y. Daoud, N. Abdellatif and T. Sari, A mathematical model of anaerobic digestion with syntrophic relationship, substrate inhibition and distinct removal rates, *SIAM J. Appl. Dyn. Syst. SIADS*, 20:3, pages 1621–1654, 2021.

S. Nouaoura, N. Abdellatif, R. Fekih-Salem and T. Sari Mathematical analysis of a three-tiered model of anaerobic digestion. *SIAM - Journal on Applied Mathematics (SIAP)*, 81:3, pages 1264–1286, 2021.

S. Nouaoura, R. Fekih-Salem, N. Abdellatif and T. Sari, Mathematical analysis of a three-tiered food-web in the chemostat, *Discrete & Contin. Dyn. Syst. Ser. B*, 26:10, pages 5601–5625, 2021.

S. Nouaoura, R. Fekih-Salem, N. Abdellatif and T. Sari, Operating diagrams for a three-tiered microbial food web in the chemostat, https://hal.archives-ouvertes.fr/hal-03284354, 2021.

T. Sari, M. El-Hajji and J. Harmand, The mathematical analysis of a syntrophic relationship between two microbial species in a chemostat, *Math. Biosci. Eng. J*, 9, pages 627–645, 2012.

T. Sari and M.J. Wade, Generalised approach to modelling a three-tiered microbial food-web, *Math. Biosci. J*, 291: pages 21–37, 2017.

S. Sobieszek, M.J. Wade and G.S.K. Wolkowicz, Rich dynamics of a three-tiered anaerobic food-web in a chemostat with multiple substrate inflow, *Math. Biosci. Eng. J*, 17: pages 7045–7073, 2020.

M.J. Wade, R.W. Pattinson, N.G. Parker and J. Dolfing, Emergent behaviour in a chlorophenol-mineralising three-tiered microbial "food web", *Theor. Biol. J*, 389: pages 171–186, 2016.

A. Xu, J. Dolfing, T.P. Curtis, G. Montague and E. Martin, Maintenance affects the stability of a two-tiered microbial "food chain"?, *Theor. Biol. J*, 276: pages 35–41, 2011.